coatings

MDPI

Article

Josephson dc Current through T-Shaped Double-Quantum-Dots Hybridized to Majorana Nanowires

Hairui Zhang [1,*], Lianliang Sun [2] and Jia Liu [3]

[1] Department of Environmental Engineering, Hohhot Minzu College, Hohhot 010050, China
[2] College of Science, North China University of Technology, Beijing 100144, China
[3] School of Science, Inner Mongolia University of Science and Technology, Baotou 014010, China
* Correspondence: hxyhjxy@imnc.edu.cn

Abstract: We study quantum interference effects on Josephson current in T-shaped double quantum dots (TDQDs) with one of them (the central dot) is sandwiched between the left and right topological superconductor nanowires hosting Majorana bound states (MBSs). We find that the current's magnitude is suppressed by the inter-dot coupling that induces the quantum interference effect, with unchanged jump in the current at particular phase difference between the two nanowires from which the Josephson effect arises. The current remains as a sinusoidal function with respective to the phase difference in the presence of quantum interference effect, but with significant reduction. The central broad peak in the curve of the Josephson current versus the QDs' levels are split in different ways depending on the configurations of the latter. We also find that the impacts of the non-z-axial direction magnetic field, bending angle between the two nanowires and the direct hybridization amplitude between the MBSs on the current all depend on the arrangement of the QDs' energy levels.

Keywords: Josephson current; quantum dots; Majorana nanowires; quantum interference

check for updates

Citation: Zhang, H.; Sun, L.; Liu, J. Josephson dc Current through T-Shaped Double-Quantum-Dots Hybridized to Majorana Nanowires. *Coatings* **2023**, *13*, 523. https://doi.org/10.3390/coatings13030523

Academic Editor: Emerson Coy

Received: 28 November 2022
Revised: 18 February 2023
Accepted: 20 February 2023
Published: 27 February 2023

1. Introduction

In recent years, extensive investigations were devoted to the Josephson current flowing through hybridized structures composing of quantum dots (QDs) sandwiched between superconductors (S-QDs-S) [1–4]. In such kind of Josephson junction, Andreev reflection processes take place at the interfaces between the QDs and the superconductors characterized by converting an electron (a hole) into a hole (an electron) [4,5]. The electron and hole on the QDs are then coherently coupled to each other and form the Andreev bound states which are entangled time-reversed electron-hole Kramers pairs [4–6]. They have quantized energy levels positioned near the Fermi level in-between the energy-gap of the superconductors, and carry Josephson current (supercurrent) if the phases of the two supercoductors are different from each other [4]. The Josephson effect is attractive in designing various phase-coherent electronic devices, such as Josephson field-effect transistors [7,8]. Josephson diode [9]. Josephson sensors for detecting ultra-weak magnetic fields or electromagnetic radiation, and ultrafast digital quantum circuits [10]. This effect is also fascinating in manipulation of phase-dependent heat currents [11], including thermal rectifiers [12,13], heat engines [14], thermometers [15], and thermal transistors [16], and so on.

Since the electron-hole pairs are neutral in charge, researchers then have been naturally trying to prepare and manipulate Majorana bound states (MBSs) in superconductors during the last two decades [17]. This is mainly because that the MBSs are solid state quasiparticles of Majorana fermions. They are of their own antiparticles and zero in charge and energy, which are similar to the electron-hole pairs in superconductors. Due to these exotic properties, the MBSs have been one of the focuses of recent experimental and theoretical efforts in condensed matter physics [18–20]. Many applications of the MBSs were proposed, such as in fault-tolerant quantum computation [18], spintronics [21], and thermoelectricity [22–24]. Fu and Kane [25] theoretically predicted in 2008 that the MBSs can be realized in a kind of topological superconductor nanowire with strong Rashaba spin-orbit interaction in proximity with an s-wave superconductor under a strong Zeeman field. Many subsequent investigations have proved that nonlocal MBSs can been realized in various Josephson junctions [26–30]. The currently mainstream technique for detecting the MBSs is by transport measurements with the help of a tunneling contact [19]. The MBSs induce resonant Andreev reflection which arises an zero-bias abnormal peak in the electronic differential conductance. This phenomenon has been experimentally demonstrated on Majorana nanowires having strong spin-orbit interaction. Another kind of effective detection scheme for the MBSs is by using Josephson junctions composing of two topological superconductors, each of which hosts a pair of Majorana modes at its opposite ends [26–30]. The MBSs on the two nanowires interact with each other and form a single Andreev bound state whose energy is related to the phase difference between the two superconductors, and carries supercurrent from one superconductor to the other. Correspondingly, there was much work devoted to Josephson current through a QD sandwiched between semiconductor nanowires in proximity-contact with s-wave superconductors to induce the MBSs at their ends (Majorana nanowires) [31–33]. They found some extraordinary results generated by the MBSs that are quite different from those in similar system of QD connected to trivial phase superconductors. For example, large Josephson current survives when the energy level of the QD is tuned away from the Fermi energy, and oscillates with the superconductor phase difference with a fixed abrupt jump of current whenever the phase difference is $\pm\pi$ [32].

If more than one QDs are inserted between the superconductors, they provide multiple electron transport channels. In such kind of structures, interesting quantum interference effect takes place and exerts profound impacts on the Josephson current [34]. In the present manuscript, we study the supercurrent through a structure composed of T-shaped double QDs (TDQDs) and the left and right Majorana nanowires forming a Josephson junction, which is shown in Figure 1. We find that the quantum interference effect arising from inter-dot coupling does not change the current's jumps at $\pm\pi$, and induces either peak or dip in the supercurrent depending on the arrangement of the QDs' levels. The amplitude of the Josephson current can be fully adjusted with the help of bending angle between the two Majorana nanowires, in-plane magnetic fields, or the direct hybridization strength between the MBSs at the ends of each Majorana nanowires. In the applications for designing superconducting devices, it is crucial to control the current amplitude or density flowing between different junctions [35]. Especially, there is much interesting in the subject of fabricating coatings of superconductor thin films deposited on metallic or semiconductor buffer layers in recent years [36,37]. When the buffer layers between the superconductors become thin enough to exhibit quantized energy levels, it resembles the QD in our system. Therefore, our presented results may by useful in adjusting current strength in the newly developed research area of coated-superconductors [35–38].

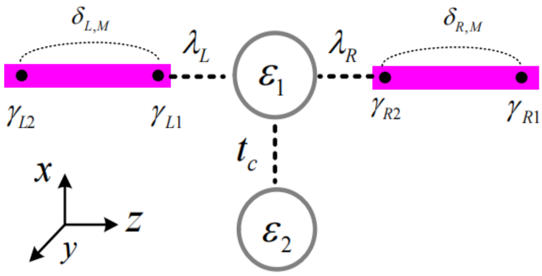

Figure 1. (Color online) Schematic plot of the studied system composed of T-shaped double quantum dots sandwiched between two nanowires hosting Majorana bound states on their ends. The coupling *strengths* between the central dot and the left/right Majorana bound states are denoted by $\lambda_{L/R}$. Due to the substrate superconductors of the nanowires, different phase factors arise in $\lambda_{L/R}$. Here we consider symmetrical phase difference $\Delta\phi$ and define $\lambda_{L/R} = \lambda_0 e^{\pm i\Delta\phi/2}$. The central and the side-coupled dots are tunnel-coupled to each other with strength of t_c, and individually have *discrete* energy levels of ε_1 and ε_2.

2. Model and Method

The total Hamiltonian of the system under investigation can be divided into three parts $H = H_{QDs} + H_M + H_T$ [32–34], in which H_{QDs} represents the TDQDs and coupling between them,

$$H_{QDs} = \sum_{i=1,2;\sigma} \varepsilon_i d^\dagger_{i\sigma} d_{i\sigma} + B_x(d^\dagger_{1\uparrow} d_{1\downarrow} + H.c) + t_c \sum_{\sigma} (d^\dagger_{1\sigma} d_{2\sigma} + H.c), \tag{1}$$

where $d^\dagger_{i\sigma}$ ($d_{i\sigma}$) is the creation (annihilation) operator of electrons having discrete energy level ε_i and spin state σ. The quantity t_c in Equation (1) is the coupling amplitude between the two *QDs*, and B_x is the strength of the magnetic field applied along x direction. The Hamiltonian H_M accounts for the left and right Majorana nanowires,

$$H_M = i \sum_{\alpha=L,R} \delta_{M,\alpha} \gamma_{\alpha 1} \gamma_{\alpha 2}, \tag{2}$$

in which $\delta_{M,L/R}$ is the hybridization amplitude between the MBSs formed at opposite ends of the left/right nanowires. The operators for the MBSs satisfy the following commutation relation $\gamma_{\alpha j} = \gamma^\dagger_{\alpha j} (j = 1,2)$ and $\{\gamma_{\alpha i}, \gamma_{\alpha' j}\} = \delta_{\alpha,\alpha'} \delta_{i,j}$. The Hamiltonian $H_T = \sum_{\alpha=L,R} H_{d\alpha}$ is for the tunneling coupling between the central QD and the left/right Majorana nanowires, with [32,33].

$$H_{d1,L} = (\lambda_L d_{1\uparrow} - \lambda^*_L d^\dagger_{1\uparrow}) \gamma_{L1}, \tag{3a}$$

$$H_{d1,R} = i[\lambda_R(\cos\frac{\theta}{2} d_{1\uparrow} + \sin\frac{\theta}{2} d_{1\downarrow}) - \lambda^*_R(\cos\frac{\theta}{2} d^\dagger_{1\uparrow} + \sin\frac{\theta}{2} d^\dagger_{1\downarrow})] \gamma_{R2}, \tag{3b}$$

in which $\lambda_{L/R}$ is the hybridization amplitude between the central QD and the left/right Majorana nanowires prepared on top the substrate s-wave superconductors. A phase factor emerges at the hybridization amplitude as $\lambda_{L/R} = \lambda_0 \exp(i\phi_{L/R}/2)$. Assuming symmetrical left/right substrate superconductors, we define $\phi_{L/R} = \pm\Delta\phi/2$ and the difference between them generates the Josephson current. The quantity θ is the mutual orientation angle between the two nanowires possibly not aligned along the same orientation. For the convenience of calculations, we convert the MBSs to regular fermion representation with the help of the following unitary transformation [33,39]: $f_{L/R} = (\gamma_{L/R1} + i\gamma_{L/R2})/\sqrt{2}$ and $f^\dagger_{L/R} = (\gamma_{L/R1} - i\gamma_{L/R2})/\sqrt{2}$.

To calculate the system's energy diagram and the Green's function related to the Josephson current in matrix form, we introduce the generalized Nambu representation as [32] $\psi^\dagger = (d^\dagger_{1\uparrow}, d^\dagger_{1\downarrow}, d_{1\downarrow}, d_{1\uparrow}, d^\dagger_{2\uparrow}, d^\dagger_{2\downarrow}, d_{2\downarrow}, d_{2\uparrow}, f^\dagger_L, f_L, f^\dagger_R, f_R)$. The transformed Hamiltonian $\tilde{H} = \frac{1}{2}\psi^\dagger H \psi$ is then written as a 12×12 matrix:

$$\tilde{H} = \begin{bmatrix} \tilde{H}_{d1} & \mathbf{t}_c & \tilde{H}_{d1,L} & \tilde{H}_{d1,R} \\ \mathbf{t}_c^\dagger & \tilde{H}_{d2} & 0 & 0 \\ \tilde{H}_{L,d1} & 0 & \tilde{H}_{LL} & 0 \\ \tilde{H}_{R,d1} & 0 & 0 & \tilde{H}_{RR} \end{bmatrix}, \tag{4}$$

where the block-diagonal sub-matrixes are $\tilde{H}_{di} = \sigma_z \otimes (\varepsilon_i \sigma_z + B_x \sigma_x)$,$\mathbf{t}_c = t_c \sigma_z$,$\tilde{H}_{\alpha\alpha} = \delta_{M,\alpha}\sigma_z$, with the symbol $\otimes$ denoting the inner product of two matrixes, and σ_x, σ_z the Pauli matrixes. The sub-matrixes for the hybridization between the central dot and the Majorana nanowires satisfy $\tilde{H}_{\alpha,d1} = \tilde{H}^\dagger_{d1,\alpha}$, and their explicit forms are,

$$\tilde{H}_{L,d1} = \frac{\sqrt{2}}{2}\begin{bmatrix} -\lambda_L^* & 0 & 0 & \lambda_L \\ -\lambda_L^* & 0 & 0 & \lambda_L \end{bmatrix}, \tag{5a}$$

$$\tilde{H}_{R,d1} = \frac{\sqrt{2}}{2}\begin{bmatrix} \lambda_R \cos\frac{\theta}{2} & \lambda_R \sin\frac{\theta}{2} & \lambda_R^* \sin\frac{\theta}{2} & \lambda_R^* \cos\frac{\theta}{2} \\ -\lambda_R \cos\frac{\theta}{2} & -\lambda_R \sin\frac{\theta}{2} & -\lambda_R^* \sin\frac{\theta}{2} & -\lambda_R^* \cos\frac{\theta}{2} \end{bmatrix}. \tag{5b}$$

The dc Josephson current arisen from phase difference between the left and right substrate superconductors $\Delta\phi$ is calculated from the nonequilibrium Green's function technique as [32,40],

$$J = \frac{e}{h}\int d\varepsilon \mathrm{ReTr}[\tilde{\sigma}_z(\tilde{\Sigma}^a G^a_{d1} - \tilde{\Sigma}^r G^r_{d1})] f(\varepsilon), \tag{6}$$

where the 4×4 matrix $\tilde{\sigma}_z = \sigma_z \otimes \mathbf{1}_{2\times 2}$. The quantity $\tilde{\Sigma}^{r/a} = \Sigma^{r/a}_L - \Sigma^{r/a}_R$ represents the difference between the self-energies contributed from the left and right Majorana nanowires, with $\Sigma^{r/a}_\alpha = \tilde{H}_{d1,\alpha} g^{r/a}_\alpha \tilde{H}_{\alpha,d1}$. The retarded/advanced Green's function of the α-th Majorana nanowires free from coupling to the QDs is $g^{r/a}_\alpha = [\varepsilon - H_\alpha \pm i0^+]^{-1}$. The retarded/advanced Green's function of the central QD in the expression of the dc Josephson current is given by $G^{r/a}_{d1} = [\varepsilon \mathbf{1}_{4\times 4} - \tilde{H}_{d1} - \mathbf{t}_c^\dagger \tilde{H}_{d2} \mathbf{t}_c - (\Sigma^{r/a}_L + \Sigma^{r/a}_R)]^{-1}$. In Equation (6), $f(\varepsilon) = 1/[1 + \exp(\varepsilon/k_B T)]$ is the equilibrium Dirac-Fermi distribution function, with k_B the Boltzmann constant and T the system's equilibrium temperature which is set to be zero in numerical calculations.

3. Numerical Results

In the following numerical investigations, we fix the value of $\lambda_0 = 1$ as the energy unit and set $\delta_{M,L} = \delta_{M,R} = \delta_M$. We focus our attention on impacts of the quantum interference effects on the dc Josephson current mainly under three different cases: identical dots' levels $\varepsilon_1 = \varepsilon_2$; varying ε_1 with fixed ε_2; and varying ε_2 with certain value of ε_1. We emphasize that the dots' levels can be fully adjusted via gate voltages in experiments. We fist present the Josephson current varying with respective to the phase difference $\Delta\phi$ for identical dots' levels $\varepsilon_1 = \varepsilon_2 = 0$ in Figure 2a and $\varepsilon_1 = \varepsilon_2 = \lambda_0$ in Figure 2d with different values of the inter-dot coupling strength t_c. When the central dot is disconnected from the other dot ($t_c = 0$), the current in Figure 2a has a triangle line-shape in the regimes of both $0 < \Delta\phi < \pi$ and $\pi < \Delta\phi < 2\pi$. It shows a discontinuous jump at $\Delta\phi = \pi$. This result is in consistent with that in refs. [32,34]. Turing on the coupling between the two dots ($t_c \neq 0$), the Josephson current exhibits a sinusoidal function form with respective to $\Delta\phi$ [32–34], and the jump from positive to negative value at $\Delta\phi = \pi$ remains unchanged. These two main features of the Josephson current are robust against the value of inter-dot coupling in a large regime ($0 \leq t_c \leq \lambda_0$ as in the figure). Meanwhile, the magnitude of the Josephson current is obviously weakened with increasing t_c, which is similar to the results in the structure of the TDQDs sandwiched between two superconductor leads [34]. To explain the properties of the Josephson current, we show the energy diagram of the system calculated from the

Hamiltonian in Equation (4). Figure 2b for the case of $t_c = 0$ shows the obvious zero-energy crossing points when the phase difference is $\Delta\phi = \pi$, where the current $J \sim \partial E^{\pm}/\partial\Delta\phi$ is zero and changes its sign. The quantity $E^{\pm}$ in the above expression are the Andreev bound states which are paired with energy of opposite signs. Note that in the case of $t_c = 0$, the properties of the Josephson current in Figure 2a and the associated Andreev bound states in Figure 2b are consistent with those in ref. [32], but is quite different from that in ref. [34] in which the dot is coupled to superconductor leads. In the presence of interdot coupling $t_c = 0.5\lambda_0$ in Figure 2c, we find that two new states emerge at $\varepsilon = \pm t_c$ which is also very different from that in ref. [34]. Correspondingly, the current's magnitude in Figure 2a is suppressed due to the gap between the Andreev bound states induced by interaction between the two dots.

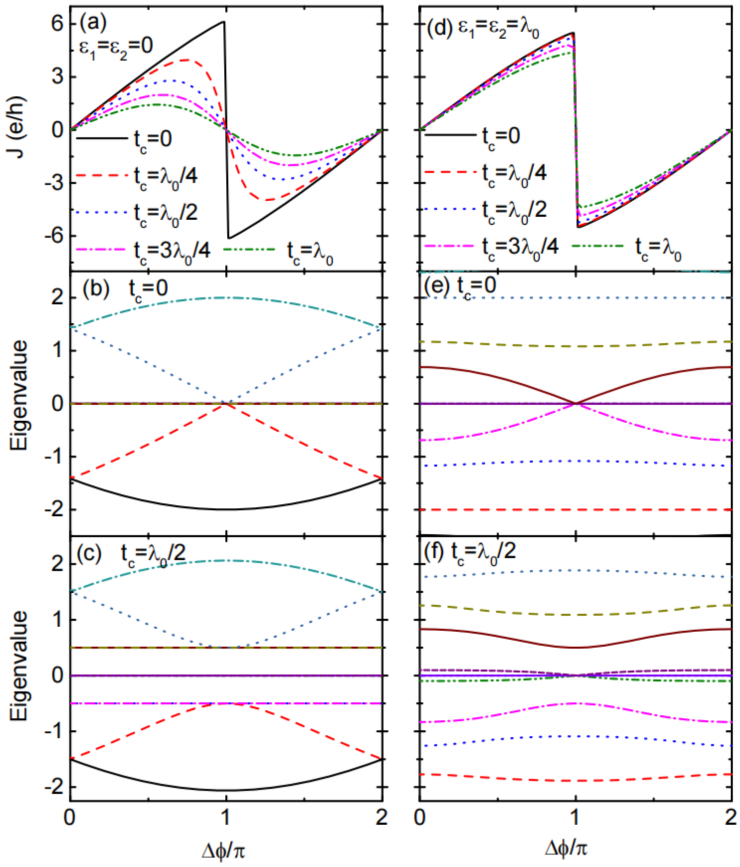

Figure 2. (Color online) Josephson current in (**a**,**d**) and the associated in-gap energy diagram in (**b**,**c**,**e**,**f**) versus the phase difference between the left and right Majorana nanowires for different values of inter-dot coupling strength t_c and QDs' levels. Other parameters are $\theta = 0$, $\delta_M = 0$, and $B_x = 0$.

For the straight left and right Majorana nanowires ($\theta = 0$) in the absence of the magnetic field ($B_x = 0$), the analytical expressions of the Green's function can be obtained as,

$$G^r_{d1} = \begin{bmatrix} \varepsilon_- - 2M & -2iM\sin\frac{\Delta\phi}{2} \\ 2iM\sin\frac{\Delta\phi}{2} & \varepsilon_+ - 2M \end{bmatrix}^{-1}, \tag{7}$$

where $M = \lambda_0^2/(\varepsilon^2 - \delta_M^2 + i0^+)$, and $\varepsilon_\pm = \varepsilon \pm \varepsilon_1 - t_c^2/(\varepsilon \pm \varepsilon_2 + i0^+) + i0^+$. The Josephson current then is reduced to,

$$J = -4\sin\Delta\phi \frac{e}{h}\int_{-\infty}^{0} \frac{\mathrm{Re}(M^2)}{|G_{d1}^r|^2} d\varepsilon, \tag{8}$$

from which it is clear that the sinusoidal relationship between the Josephson current and the phase difference $\Delta\phi$ is unchanged by the values of t_c or the dots' levels $\varepsilon_{1(2)}$. As is shown in Figure 2d, the magnitude of the Josephson current only changes by a little amount with varying t_c for the non-zero dots' levels, which is similar to the results in ref. [32]. The reason is that the crossing points of the Andreev bound states always survive in Figure 2e,f. Importantly, Figure 2d indicates that the Josephson current is quite strong even when the dots' levels are apart from the Fermi level $\mu = 0$, a result that is different from the structure if the central QD being sandwiched between the left and right normal (trivial) superconductors. This indicates that a nontrivial phase of the Majorana nanowires is induced by the superconductor-proximity effect, from which the Josephson current arises.

Since the sinusoidal line-shape of the Josephson current varying with the phase difference survives regardless of the value of phase difference, in the following numerical calculations we fix $\Delta\phi = \pi/2$ and study the influences of some other quantities, including the bending angle θ between the two nanowires, magnetic field B_x and direct Majorana hybridization amplitude δ_M, on the properties of the Josephson current. In Figure 3 we display the current under the condition of identical QDs' levels $\varepsilon_1 = \varepsilon_2$. Figure 3a shows that the broad peak in J centered at $\varepsilon_{1(2)} = 0$ is lowered and split into two, whose positions are individually at $\varepsilon_{1(2)} = \pm t_c$. This happens at relatively small value of the inter-dot coupling, $t_c \leq \lambda_0/2$. With even increasing t_c, the peaks in the current are emerged into a dip at $\varepsilon_{1(2)} = 0$. The reason is that the gap opened by the inter-dot coupling t_c becomes too wide to be overcome and then the current is obviously suppressed. Figure 3b displays the impacts of the bending angle θ on the Josephson current for fixed value of $t_c = \lambda_0/2$. For the straight Majorana nanowire-QDs-Majorana nanowire set-up ($\theta = 0$), the MBSs at the ends of the Majorana nanowirez couple only to one certain spin state (for example spin-up electrons) in the QDs due to the helical property of the MBSs. The Josephson current exhibits the double-peak configuration around the Fermi level $\varepsilon_{1(2)} = 0$ as indicated by the solid line in Figure 3b. This result is quite different from those in ref. [32] where only one QD is sandwiched between the Majorana nanowires. For $\theta \neq 0$, i.e., the two Majorana nanowires are not straight with respective to the QDs, now the MBSs will interact to both spin-up and spin-down electrons on the QDs, and is anticipated to modulate the behavior of the Josephson current, which is significantly suppressed in the whole QDs' levels regime. Meanwhile, the double-peak configuration is mainly retained with increasing θ, but their positions and height are all changed. When the two Majorana nanowires are rotated to the same side of the central QD and in parallel to each other ($\theta = \pi$), the Josephson current is completed blockaded $J \equiv 0$ because now the MBSs in the two nanowires are totally decoupled [41]. This result is also in consistent with that in ref. [32]. Figure 3c shows the influences of the direct hybridization between the MBSs on the Josephson current. It indicates that MBS-MBS interaction induces another pair of peaks in J even for a very small value, for example the dashed line in Figure 3c in which $\delta_M = 0.1\lambda_0$. For sufficiently large value of δ_M the two peaks induced by t_c are broadened, but those from the inter-MBSs coupling clearly show them at $\varepsilon_{1(2)} = \pm\delta_M$, see the dash-dot-dot green line for $\delta_M = \lambda_0$. Our result indicates that the direct overlap between the MBSs plays similar roles as those in the structure when a QD is coupled to normal metal leads and side-coupled to MBSs [39].

We then study in Figure 4 the cases of different QDs' levels. As is shown in Figure 4a,b, the Josephson current as a function of ε_1 has a broad Lorentz peak centered at $\varepsilon_1 = 0$. Such a character is robust against the value of inter-dot coupling t_c in Figure 4a and ε_2 in Figure 4b. For a fixed $\varepsilon_2 = 0$ in Figure 4a, the magnitude of J is monotonously suppressed by increasing t_c. When the energy level of the side-coupled dot ε_2 is shift away from the Fermi level $\mu = 0$, Figure 4b shows that J is obviously enhanced. The above features of the current are in consistent with those in Figure 2 and can be explained by the associated energy diagram. The current varying with respective to ε_2 in Figure 4c,d is quite different from that in Figure 4a,b. The most prominent change is that now the current develops a pair of peaks in the presence of quantum interference effect ($t_c \neq 0$). Meanwhile, the magnitude of the current is significantly suppressed by either t_c or ε_2. It indicates that the side-coupled dot mainly exerted its impacts around the Fermi level $\mu = 0$, due to the zero-energy character of the MBSs. Interestingly, the positions of the double peaks around the Fermi level are quite stable regardless of the change of t_c in Figure 4c and ε_1 in Figure 4d, which may find use in detecting the existence of the MBSs. Here we emphasize the above results are quite different from those in ref. [34], in which the Josephson current exhibits Fano line-shape by varying the QDs' levels. In Figure 4 of the present paper, however, the Josephson current shows respectively a single- and double-peak configuration by varying ε_1 and ε_2. The difference between the present work and ref. [34] originates from the difference between the leads coupled to the QD.

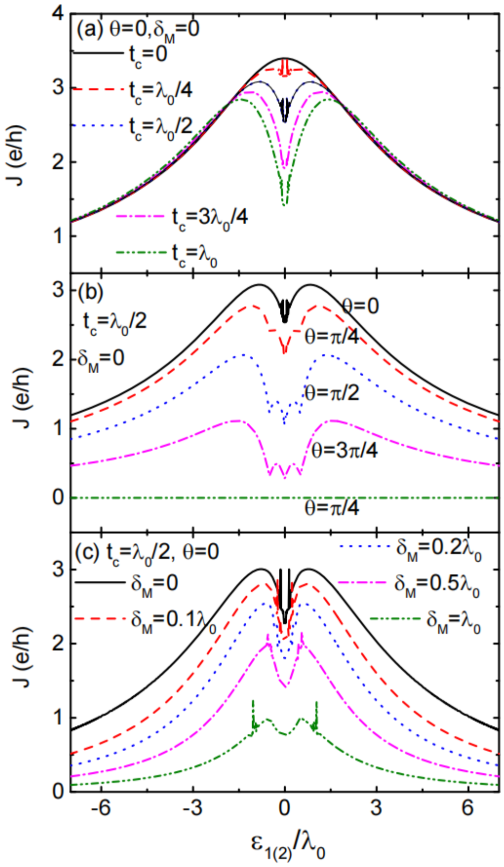

Figure 3. (Color online) Josephson current as a function of identical QDs' levels $\varepsilon_1 = \varepsilon_2$ for fixed $\Delta\phi = \pi/2$ and different values of t_c in (**a**), θ in (**b**) and δ_M in (**c**). Other parameters are shown in the figures.

Figure 5 shows the behavior of the Josephson current varying as a function of ε_1 in (a), (b) and ε_2 in (c) and (d) under different values of bending angle θ and Majorana interaction δ_M, respectively. Similar to the case in Figure 3b, the magnitude of the current in Figure 5a is monotonously suppressed by increasing θ. The broad peak in J when $\theta = 0$ evolves into a dip when $\theta > \pi/4$. The reason is that the MBSs at the ends of the Majorana nanowires will interact to both spin-up and spin-down electrons on the QDs as $\theta \neq 0$, and then their impacts are strengthened. Because of the zero-energy nature of the MBSs, the current around $\varepsilon_1 = 0$ is more sensitive to the change of θ and then a dip is induced. In experiments, the MBSs prepared at opposite ends of a Majorana nanowire may interact to each other, whose strength depends on the length of the nanowire. The direct hybridization between the MBSs splits the peaks in the linear conductance or density of states of a QD sandwiched between two normal metal leads [35], but not the Josephson current in the present work. It also exerts significant influences on some other transport quantities, such as the sign change or abnormal enhancement of the thermopower that can be used for detecting the existence of MBSs [22–24]. Figure 5b shows that the current is obviously reduced. We attribute this change of the current to the fact that the zero-energy Majorana state is destroyed by the MBS-MBS interaction. It indicates that to generate a larger Josephson current, one should elongate the nanowire. The line-shape of the current varying as a function of ε_2 is similar to that in Figure 4c,d. When $\theta = 0$, the double peaks around $\varepsilon_2 = 0$ in Figure 5c disappear and the current develops a dip therein, accompanied by a strong reduction of the current. With increasing δ_M the current is suppressed with almost unchanged peak configuration.

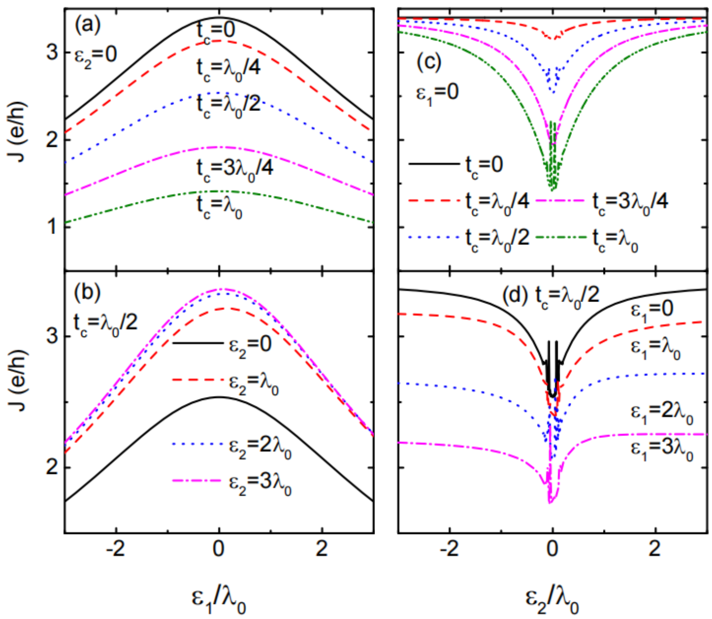

Figure 4. (Color online) Josephson current varying with respective to ε_1 in (**a**) for fixed ε_2 and different t_c, and in (**b**) for fixed $t_c = \lambda_0/2$ and different ε_2. Similar cases are shown in (**c**,**d**) for $J - \varepsilon_2$.

In experiments, a strong magnetic field is required to induce the MBSs at the ends of the Majorana nanowires. It will unavoidably leak into the QDs and changes the transport processes in a nonnegligible way. The magnetic field along the z axis induces the usual Zeeman splitting of the QDs' levels, whereas that along the x or y axis will make the MBSs to hybridize with both spin-up and spin-down electrons on the QDs, which is similar to the function of the mutual angle between the two Majorana nanowires. As a result of it, the current's magnitude in Figure 6 is reduced under both of the three different arrangements of QDs' levels. For the case of $\varepsilon_1 = \varepsilon_2$, Figure 6a shows that the double-peak configuration of the current is retained, with the emergence of a pair of dips. The peak in Josephson current evolves into a broad valley with increasing B_x at $\varepsilon_1 = 0$ in Figure 6b, which is in consistent with the results in Figure 5a, and also in Ref. [32]. For a fixed $\varepsilon_1 = 0$ and varying ε_2, the magnitude of the current in the regimes of $|\varepsilon_2| > t_c$ is significantly suppressed whereas the peaks around $\varepsilon_2 = \pm t_c$ is well preserved. The changes of the Josephson current can be attributed to the enhanced impacts of the MBSs when both of the two spin states of electrons on the QDs are coupled to them via the magnetic field along the x axis. Finally, we emphasize that there are surface traps in the nanowires whose impacts on the current are neglected in the present study. This is mainly because that the surfaces may change the energy states and the coupling strength between the nanowire and the QD, which should not change the qualitative results due to the MBSs, as long as they survives against the traps.

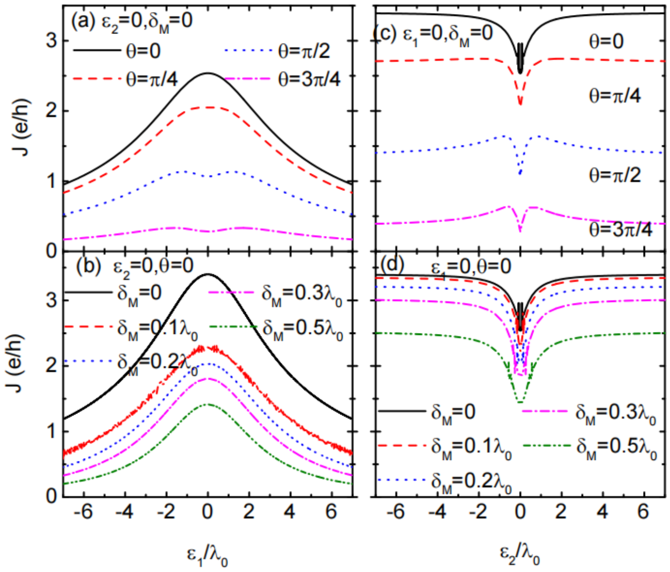

Figure 5. (Color online) Behaviors of the Josephson current as a function of ε_1 in (**a**) for different θ and in (**b**) for different δ_M. Similar cases of the current versus ε_2 are given in (**c**,**d**). Except the parameters shown in the figures, the value of $\Delta\phi$ is fixed at $\pi/2$.

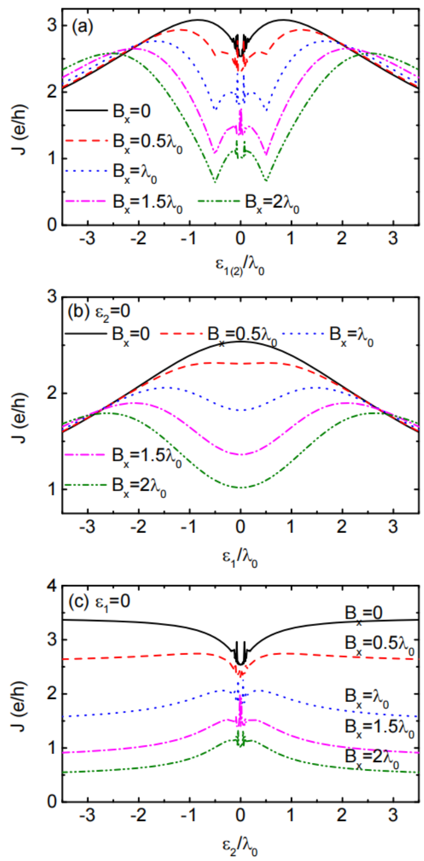

Figure 6. (Color online) Effects of the junction bending on the Josephson current varying with respective to $\varepsilon_1 = \varepsilon_2$ in (**a**), ε_1 in (**b**) for $\varepsilon_2 = 0$, and ε_2 in (**c**) for $\varepsilon_1 = 0$. Other parameters are $\Delta\phi = \pi/2$, $t_c = \lambda_0/2$ and $\theta = \delta_M = 0$.

4. Summary

In summary, we have studied the Josephson current through TDQDs connected to the left and right Majorana nanowires. It is found that the jumps in the current at $\Delta\phi = \pm\pi$, where $\Delta\phi$ is the phase difference between the two nanowires, survives in the presence of quantum interference effects arisen from inter-dot coupling. The Josephson current around the Fermi level, which is set to be zero, is sensitive to the quantum interference effect, as well as parameters related to the MBSs, including the bending angle between the two Majorana nanowires, the direct hybridization amplitude between the two modes of the MBSs, or the magnetic fields applied on the Majorana nanowires. In addition, by adjusting the QDs' energy levels, the osephson current around the Fermi level can be either suppressed or enhanced. The present results provides an efficient way of manipulating the Josephson current coherently by means of the quantum interference effect. Our results may be applied in adjusting current amplitude or density in the rapidly developing coated-superconductor technologies.

Author Contributions: Writing—original draft preparation, H.Z., J.L. and L.S.; writing—review and editing, H.Z., J.L. and L.S. All authors have read and agreed to the published version of the manuscript.

Funding: This work was supported by the Program for 2022 Fundamental Research Funds for the colleges and universities directly under Inner Mongolia Autonomous Region; R&D Program of Beijing Municipal Education Commission (KM201910009002) and National Natural Science Foundation of China under Grant No. 12264037.

Institutional Review Board Statement: Not applicable.

Informed Consent Statement: Not applicable.

Data Availability Statement: All data included in this study are available upon request by contact with the corresponding author.

Conflicts of Interest: The authors declare no conflict of interest.

References

1. Sun, Q.F.; Wang, J.; Lin, T.H. Photon-assisted Andreev tunneling through a mesoscopic hybrid system. *Phys. Rev. B* **1999**, *59*, 13126. [CrossRef]
2. Sun, Q.F.; Wang, J.; Lin, T.H. Control of the supercurrent in a mesoscopic four-terminal Josephson junction. *Phys. Rev. B* **2000**, *62*, 648. [CrossRef]
3. Tkachov, G.; Richter, K. Effect of magnetic pair breaking on Andreev bound states and resonant supercurrent in quantum dot Josephson junctions. *Phys. Rev. B* **2007**, 75, 134517. [CrossRef]
4. Rodero, A.M.; Yeyati, A.L. Josephson and Andreev transport through quantum dot. *Adv. Phys.* **2011**, 60, 899. [CrossRef]
5. Pala, M.G.; Governale, M.; Konig, J. Nonequilibrium Josephson and Andreev current through interacting quantum dots. *New. J. Phys.* **2007**, *9*, 278. [CrossRef]
6. Oguri, A.; Tanaka, Y.; Bauer, J. Interplay between Kondo and Andreev-Josephson effects in a quantum dot coupled to one normal and two superconducting leads. *Phys. Rev. B* **2013**, *87*, 075432. [CrossRef]
7. Doh, Y.J.; Van Dam, J.A.; Roest, A.L.; Bakkers, E.P.A.M.; Kouwenhoven, L.P.; De Franceschiy, S. Tunable Supercurrent Through Semiconductor Nanowires. *Science* **2005**, *309*, 272–275. [CrossRef]
8. Herrero, P.J.; van Dam, J.; Kouwenhoven, L.P. Quantum supercurrent transistors in carbon nanotubes. *Nature* **2006**, *439*, 953. [CrossRef]
9. Gino, V.G.; Gupta, M.; Pendharkar, M.; Dong, J.T.; Dempsey, C.P.; Palmstrm, C.; Pribiag, V.S. Selective control of conductance modes in multi-terminal Josephson junctions. *Nat. Commun.* **2022**, *13*, 5933. [CrossRef]
10. Soloviev, I.I.; Schegolev, A.E.; Klenov, N.V.; Bakurskiy, S.V.; Kupriyanov, M.Y.; Tereshonok, M.V.; Shadrin, A.V.; Stolyarov, V.S.; Golubov, A.A. Adiabatic superconducting artificial neural network: Basic cells. *J. Appl. Phys.* **2018**, *124*, 152113. [CrossRef]
11. Seja, K.M.; Jacob, L.; Lofwander, T. Thermopower and thermophase in a d-wave superconductor. *Phys. Rev. B* **2022**, *105*, 104506. [CrossRef]
12. Martnez-Perez, M.J.; Giazotto, F. Efficient phase-tunable Josephson thermal rectifier. *Appl. Phys. Lett.* **2013**, *102*, 182602. [CrossRef]
13. Martnez-Perez, M.J.; Fornieri, A.; Giazotto, F. Rectification of electronic heat current by a hybrid thermal diode. *Nat. Nanotech.* **2015**, 10, 303. [CrossRef] [PubMed]
14. Hofer, P.P.; Souquet, J.R.; Clerk, A. Quantum heat engine based on photon-assisted Cooper pair tunneling. *Phys. Rev. B* **2016**, *93*, 041418. [CrossRef]

15. Giazotto, F.; Solinas, P.; Braggio, A.; Bergeret, F.S. Ferromagnetic-Insulator-Based Superconducting Junctions as Sensitive Electron Thermometers. *Phys. Rev. Appl.* **2015**, *4*, 044016. [CrossRef]
16. Bobkova, I.V.; Bobkov, A.V.; Silaev, M.A. Magnetoelectric effects in Josephson junctions. *J. Phys. Condens. Matter* **2022**, *34*, 353001. [CrossRef]
17. Qi, X.L.; Zhang, S.C. Topological insulators and superconductors. *Rev. Mod. Phys.* **2011**, *83*, 1057. [CrossRef]
18. Alicea, J.; Oreg, Y.; Refael, G. Non-abelian statistics and topological quantum information processing in 1d wire networks. *Nat. Phys.* **2011**, *7*, 412. [CrossRef]
19. Mourik, V.; Zuo, K.; Frolov, S.M. Signatures of majorana fermions in hybrid superconductor-semiconductor nanowire devices. *Science* **2012**, *336*, 1003. [CrossRef]
20. Feng, G.H.; Zhang, H.H. Probing robust majorana signatures by crossed andreev reflection with a quantum dot. *Phys. Rev. B* **2022**, *105*, 035148. [CrossRef]
21. Liu, X.; Li, X.; Deng, D.L.; Liu, X.J.; Das, S.D. Majorana spintronics. *Phys. Rev. B* **2016**, *94*, 014511.[CrossRef]
22. Lopez, R.; Lee, M.; Serra, L.; Lim, J. Thermoelectrical detection of majorana states. *Phys. Rev. B* **2014**, *89*, 205418. [CrossRef]
23. Hong, L.; Chi, F.; Fu, Z.G.; Hou, Y.F.; Wang, Z. Large enhancement of thermoelectric effect by majorana bound states coupled to a quantum dot. *J. Appl. Phys.* **2020**, *127*, 124302. [CrossRef]
24. Chi, F.; Fu, Z.G.; Liu, J.; Li, K.; Wang, Z.; Zhang, P. Thermoelectric effect in a quantum dot side-coupled to majorana bound states. *Nanoscale Res. Lett.* **2020**, *15*, 79. [CrossRef] [PubMed]
25. Fu, L.; Kane, C.L. Superconducting proximity effect and Majorana fermions at the surface of a topological insulator. *Phys. Rev. Lett.* **2008**, *100*, 096407. [CrossRef]
26. San-Jose, P.; Prada, E.; Aguado, R. ac josephson effect in finite-length nanowire junctions with majorana modes. *Phys. Rev. Lett.* **2012**, *108*, 257001. [CrossRef] [PubMed]
27. Ricco, L.S.; de Souza, M.; Figueira, M.S. Spin-dependent zero-bias peak in a hybrid nanowire-quantum dot system: Distinguishing isolated majorana fermions from Andreev bound states. *Phys. Rev. B* **2019**, *99*, 155159. [CrossRef]
28. Tang, H.Z.; Zhang, Y.T.; Liu, J.J. Josephson current through a quantum dot molecule with a Majorana zero mode and Andreev bound states. *Phys. Lett. A* **2018**, *382*, 991. [CrossRef]
29. Wu, B.H.; Hassan, S.A.; Xu, X.F.; Wang, C.R. Quantum transport of planar Josephson junctions with Majorana bound states. *Phys. Rev. B* **2020**, *102*, 085414. [CrossRef]
30. Choi, S.J.; Calzona, A.; Trauzettel, B. Majorana-induced DC Shapiro steps in topological Josephson junctions. *Phys. Rev. B* **2020**, *102*, 140501(R). [CrossRef]
31. Gong, W.J.; Gao, Z.; Shan, W.F.; Yi, G.Y. Influence of an embedded quantum dot on the Josephson effect in the topological superconducting junction with Majorana doublets. *Sci. Rep.* 2016, 6, 23033. [CrossRef] [PubMed]
32. Xu, L.T.; Li, X.Q.; Sun, Q.F. Majorana dc Josephson current mediated by a quantum dot. *J. Phys. Condens. Matter* **2017**, *29*, 195301. [CrossRef] [PubMed]
33. Stefanski, P. Properties of the Majorana-state tunneling Josephson junction mediated by an interacting quantum dot. *J. Phys. Condens. Matter* **2019**, *31*, 185301. [CrossRef]
34. Cheng, S.G.; Sun, Q.F. Josephson current transport through T-shaped double quantum dots. *J. Phys. Condens. Matter* **2008**, *20*, 505202. [CrossRef]
35. Thimont, Y.; Xing, Y.T.; Bernstein, P.; Miryala, M.; Noudem, J. Joining Superconducting MgB2 Parts by Spark Plasma Sintering: A New Technique with High Potential for Manufacturing Future Superconducting Devices. *Coatings* **2022**, 12, 1151. [CrossRef]
36. Meeka, T.T.; Kobayashib, A.; Herbertc, E.; White, R.L. Superconductive coatings fabricated via external injection into a d.c. plasma. *Vacuum* **2002**, 65, 409. [CrossRef]
37. Kesgin, I.; Khatri, N.; Liu, Y.H.; Delgado, L.; Galstyan, E.; Selvamanickam, V. Influence of superconductor film composition on adhesion strength of coated conductors. *Supercond. Sci. Technol.* **2016**, 29, 015003. [CrossRef]
38. Jiang, G.; Zhao, Y.; Zhu, J.; Hong, Y.; Chen, S.; Chen, S.; Wu, Y.; Zhen, S.; Yao, L.; Hong, Z.; et al. Recent development and mass production of high Je 2G-HTS tapes by using thin hastelloy substrate at Shanghai Superconductor Technology. *Supercond. Sci. Technol.* **2020**, 33, 074005. [CrossRef]
39. Liu, D.E.; Baranger, H.U. Detecting a majorana-fermion zero mode using a quantum dot. *Phys. Rev. B* **2011**, *84*, 201308R. [CrossRef]
40. Zhu, Y.; Sun, Q.F.; Lin, T.H. Andreev bound states and the -junction transition in a superconductor/quantum-dot/superconductor system. *J. Phys. Condens. Matter* **2001**, *13*, 8783. [CrossRef]
41. Flensberg, K. Tunneling characteristics of a chain of Majorana bound states. *Phys. Rev. B* **2010**, *82*, 180516(R). [CrossRef]